Proc. Natl. Acad. Sci. USA
Vol. 93, pp. 3886–3891, April 1996
Cell Biology

Movement of yeast cortical actin cytoskeleton visualized *in vivo*

(*Saccharomyces cerevisiae*/green fluorescent protein/protein fusions/Sac6p fimbrin/Abp1p)

TIM DOYLE AND DAVID BOTSTEIN

Department of Genetics, Stanford University Medical Center, 300 Pasteur Drive, Stanford, CA 94305-5120

Contributed by David Botstein, December 29, 1995

ABSTRACT **Fusion proteins between the green fluorescent protein (GFP) and the cytoskeleton proteins Act1p (actin), Sac6p (yeast fimbrin homolog), and Abp1p in budding yeast (*Saccharomyces cerevisiae*) localize to the cortical actin patches. The actin fusions could not function as the sole actin source in yeast, but fusions between the actin-binding proteins Abp1p and Sac6p complement fully the phenotypes associated with their gene deletions. Direct observation *in vivo* reveals that the actin cortical patches move. Movement of actin patches is constrained to the asymmetric distribution of the patches in growing cells, and this movement is greatly reduced when metabolic inhibitors such as sodium azide are added. Fusion protein-labeled patches are normally distributed during the yeast cell cycle and during mating. *In vivo* observation made possible the visualization of actin patches during sporulation as well.**

The gross architecture of the actin cytoskeleton in the yeast *Saccharomyces cerevisiae* has been well characterized, although its specific cellular functions remain elusive. As visualized using fluorescently labeled phalloidin (1) or antibodies (2), the actin cytoskeleton consists of cytoplasmic actin cables and cortical actin patches whose distribution within the cell changes during the cell cycle (Fig. 1). During vegetative growth, an asymmetric distribution of these structures is apparent, with the cortical patches localizing to sites of cell surface growth and the cables often oriented toward these regions. Following entry into the cell cycle from G_0 or after G_1 phase, when the cortical patches are delocalized over the entire cell surface and the cables are distributed evenly through the cytoplasm, the cells prepare to bud. As the bud develops, most of the patches appear in the growing daughter cell, with the cables appearing to be oriented along the long axis of the mother cell. As the daughter cell matures, the patches localize to the septum, with the cables appearing to radiate from this region. During the development of mating projections in haploid cells ("shmooing"), cortical actin patches localize to the membrane of the growing tip at the site of membrane insertion (3–6).

A number of proteins have been shown to associate with the actin cytoskeleton, some specifically at the cables or patches, and some at both (reviewed in ref. 7). A great deal of effort has gone into understanding the relationships among these proteins and their roles in the functioning of the actin cytoskeleton. For example, actin has been shown to play an essential role in endocytosis involving both fimbrin (Sac6p) (8) and Sla2p (9, 10). The cortical actin patches have also been suggested to play a role in cell wall synthesis (11), whereby cell wall deposition occurs at cell membrane invaginations where the actin cytoskeleton is hypothesized to counteract the cytoplasmic turgor pressure.

The association of actin in yeast and in other organisms with dynamic activities and structures motivated us to find a way in which to observe the actin cytoskeleton in living cells to see how polymerized actin structures are redistributed during growth. The recent demonstration that the green fluorescent protein (GFP) (12, 13) from the jellyfish *Aequorea victoria* can be used as a fusion protein to mark the intracellular localization of proteins in a variety cell types (14, 15), including *Saccharomyces* (16), provided us with a means to that end.

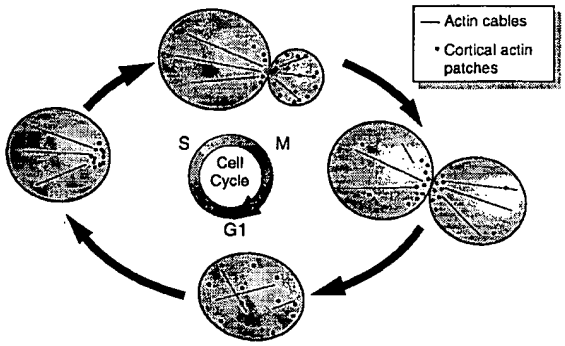

FIG. 1. Schematic representation of the distribution of the structural components of the yeast actin cytoskeleton during the cell cycle.

MATERIALS AND METHODS

Yeast Strains, Media, and Genetic Manipulations. Yeast strains are described in Table 1. Standard media, methods of cultivation, and genetic manipulation were used (19). α-Factor-induced shmooing and cell arrest were achieved by adding α-factor to an exponential culture (5×10^6 cells·ml^{-1}) to a final concentration of 20 μg·ml^{-1} (ca. 12 μM).

DNA Manipulations. Restriction endonucleases, ligase, and polymerases were purchased from New England Biolabs. Standard techniques and conditions were used (20). DNA was sequenced by the chain termination method using the modified T7 polymerase Sequenase version 2.0 (United States Biochemical).

Plasmids. Plasmids used for the expression of proteins are derivatives of pTS210 [a YCp50-based vector (21) with the *GAL1–10* promoter and *ACT1* terminator sequences replacing the *Eco*RI–*Sph* I region], which was constructed by T. Stearns (Stanford University). A short multiple cloning site separates the promoter and terminator sequences (GGATCC GC AAGCTT GC TCTAGA). *ACT1* sequences were amplified from pRB668 (a YCp50-based vector containing the 3.3-kb *Bam*HI–*Eco*RI *ACT1*-bearing chromosomal fragment). All the plasmids used here were derived from this plasmid by standard methods (20), including PCR to recover sequences encoding GFP, Act1p, Sac6p, and Abp1p. These plasmids are all nearly identical (except for fusions they encode) and are listed in Table 2. In every case, the yeast *ACT1* promoter was used, following by an entire coding sequence (including the

The publication costs of this article were defrayed in part by page charge payment. This article must therefore be hereby marked "*advertisement*" in accordance with 18 U.S.C. §1734 solely to indicate this fact.

Abbreviations: GFP, green fluorescent protein; FITC, fluorescein isothiocyanate.

Table 1. Strain descriptions

Strain	Genotype	Ref.
DBY5532 (KWY201)	*MATa/α, ura3-52/ura3-52, leu2-3, 112/leu2-3,112, his3Δ200/his3Δ200, ade2/+, ade4/+ tub2-201(Ben^r)/+, ACT1/act1Δ::LEU2, can1-1/+*	17
FY23 × FY86	*MATa/α, ura3-52/ura3-52, leu2Δ1/leu2Δ1, trp1Δ63/+, his3Δ200/+*	Fred Winston*
DDY318	*MATα, his3Δ200, leu2-3,112, lys2-801am, ura3-52, sac6Δ::LEU2*	18
DDY319	*MATa, his3Δ200, leu2-3,112 lys2-801am, ura3-52, sac6Δ::LEU2*	18
DDY321	*MATa, his3Δ200, leu2-3,112, ura3-52, abp1-Δ2::LEU2*	18
DDY322	*MATα, his3Δ200, leu2-3,112, ura3-52, abp1-Δ2::LEU2*	18

*Harvard Medical School

initiator ATG), fused (or not) the GFP sequence, followed by the *ACT1* terminator.

Microscopy Imaging and Analysis. Exponential cultures (cell density 1×10^7–1×10^6 cells·ml^{-1}) were sampled directly from the culture tubes (5 μl) and spotted on a microscope slide and covered with a coverslip or mixed with an equal volume of molten low melt agarose (at 37°C) on a prewarmed slide, quickly covered with a coverslip, and the agarose allowed to set at room temperature. Slides were mounted on a fluorescent microscope and viewed with both Nomarski and fluorescein isothiocyanate (FITC) filtered illumination at high magnification. Fluorescent photographs were taken on Kodak T-MAX 400ASA film on a Zeiss Axioscope at ×100 magnification (Plan Neofluar 100/1.3 w/iris) using BP 450–490 exciter/BP 520–560 barrier-filtered fluorescence illumination. Exposure times of 8–15 sec were generally necessary to obtain a suitable images, and since patches are dynamic, cortical patch localization and appearance are often not as defined as apparent by direct observation.

Sequential images were obtained on a Nikon Diaphot inverted microscope at ×100 magnification (Nikorfluor 100/1.3) using either a B2 (BP450–490 excitation/LP 520 barrier) or B1e (BP 470–40 excitation/BP 520–560 barrier) FITC filter sets. Images were digitized directly from a Hamamatsu (Middlesex, NJ) C2400–08 SIT camera, attached to the side port of the microscope, by IMAGE 1 software (Universal Imaging, West Chester, PA), which also controlled FITC illumination by means of a Metaltek (Raleigh, NC) filter wheel/shutter to reduce photobleaching of the sample. Collected tagged image format file images were converted to PHOTOSHOP version 3.0 (Adobe Systems, Mountain View, CA) format on an Apple Macintosh computer using PHOTOMATIC (DayStar Digital, Flowery Branch, GA) batch processing. QUICKTIME (Apple) movies were made using Adobe PREMIER version 4.0. [Some of these movies, including those from Figs. 3 and 4, are available from the World Wide Web Botstein Lab site at Stanford University (http://www-genome.stanford.edu).

RESULTS AND DISCUSSION

Construction of Plasmids Expressing Actin–GFP Fusions. To produce an actin–GFP fusion protein that could be used to mark the actin cytoskeleton *in vivo*, we made a variety of constructs using the normal actin promoter and terminator (23) on a *URA3*-marked CEN plasmid. The actin fusion to the N terminus of the GFP that worked best was pRB2133, which contains the entire actin coding sequence, a segment in-frame encoding 10 alanine residues followed by the GFP sequence. As controls (Table 2), we used identical plasmids expressing actin alone (pRB2136), GFP alone (pRB2132), or neither (i.e., just the actin promoter and terminator joined by a short polylinker; pTS422).

Plasmids pTS422 (from T. Stearns), pRB2132, pRB2133, pRB2134, pRB2135, and pRB2136 (Table 2) were all transformed into the diploid yeast DBY5532, which is heterozygous for a deletion of the *ACT1* gene marked with an adjacent insertion of the *LEU2* gene (17). This strain offered two advantages: the transformed strain would contain two copies of the actin gene (although one may be a fusion), and tetrad analysis of spores derived from the transformants would confirm the ability of the fusions to complement the actin deletion.

Expression and Visualization of Actin–GFP Fusions in Yeast. The strain carrying pRB2133 [expressing Act1–$(Ala)_{10}$–GFP] displayed fluorescent cortical patches when visualized under the microscope with FITC filter illumination. The actin–GFP fusion protein appeared to be expressed and properly localized, displaying an asymmetric cortical patch morphology typical for actin immunofluorescence or staining with rhodamine phalloidin. By viewing cells across different focal planes under the microscope, it was apparent that the patches are restricted to the surface of the cells. Thus, by focusing across the middle of the cell, patches are only visible at the edge, whereas adjusting the focal plane to the top of the cell shows patches over the whole area of the cell in focus.

Background cytoplasmic fluorescence was very strong with pRB2135 plasmid (no alanine linker) and was still significant with the pRB2134 [Act1–$(Ala)_4$–GFP]. Consequently, pRB2133 was chosen for further investigations involving visualization, and subsequent experiments were performed with this fusion, except as noted. The control plasmids pTS422 and pRB2136, neither of which contain the GFP gene, displayed only very weak autofluorescence. However, expression of the GFP alone from plasmid

Table 2. Plasmids used in this study and their effects on cell growth

Plasmid	Insert	Complementation of gene deletion	Doubling times, hr	
			Diploid	Haploid
pTS422	None	No	1.93	1.93
pRB2132	GFP	No	1.90	1.95
pRB2133	Actin–$(Ala)_{10}$–GFP	No	1.95	1.93
pRB2134	Actin–$(Ala)_4$–GFP	No	1.97	1.94
pRB2135	Actin–GFP	No	1.92	1.98
pRB2136	Actin	Yes	1.98	2.05
pRB2138	GFP*	ND	ND	ND
pRB2139	GFP*–Abp1	Yes	ND	ND
pRB2140	GFP*–Sac6	Yes	ND	ND

ND, not determined.
*Increased fluorescence S65T mutant protein (22).

pRB2132 displayed significant general cytoplasmic fluorescence, with apparent vacuolar exclusion but no cortical patches at all (data not shown). These results allowed the preliminary conclusion that the actin–GFP fusion is properly incorporated, at least occasionally, into actin cortical patches.

Tetrad analysis of the diploid cells transformed with each of the plasmids mentioned above showed that only plasmid pRB2136, which expresses the unfused actin gene, was able to complement the chromosomal actin deletion in haploid cells. None of the actin–GFP fusion proteins was capable of complementing this deletion. Thus the actin–GFP fusion, although apparently incorporated into the cytoskeleton, cannot fully execute all the essential aspects of actin function.

To determine whether expression of GFP or actin–GFP fusions might be deleterious to cell growth, strains transformed with each of the plasmids were tested for known actin mutant phenotypes—namely temperature and/or salt sensitivity—as well as doubling times and cell viability. All transformants showed normal growth phenotype when tested either directly as diploids or as their haploid segregants (Table 2). Haploid segregants were selected with the same auxotrophic requirements to ensure valid comparisons (*TUB2-ACT1; ura3–52; leu2–3, 112; his3Δ200; ADE2; ADE4*; [plasmid::*URA3*]). These results show that the inclusion of the hybrid actin–GFP fusion has no deleterious effect on growth under ordinary circumstances. This conclusion was fortified by the observation that each of the fusion protein- expressing strains in Table 1, when observed in the fluorescence microscope, appeared to have a normal actin cortical patch distribution (data not shown; see below).

Actin–GFP Fusion Localization *in Vivo*. The gross appearance, in cells taken from exponentially growing cultures, of the GFP fluorescence in actin–$(Ala)_{10}$–GFP transformants is strongly reminiscent of that observed in fixed cells by standard fluorescent methods. As expected, we observe asymmetrical localization of the punctate fluorescent patches similar to that observed for the cortical actin patches by immunofluorescence and rhodamine phalloidin labeling during the cell cycle. Because of the agreement with the many published images of fixed cells stained with antibody or phalloidin, these observations in living cells indicate that the actin–GFP fusion is being correctly assembled in the cortical actin patches. We do not observe cables with the GFP fusion proteins; most likely this reflects low signal strength of GFP fluorescence, which has been estimated to be an order of magnitude lower than that of FITC (24).

When *MAT***a** haploid cells are growth arrested by the addition of α-factor (to 20 $\mu g \cdot ml^{-1}$), with subsequent mating projection (shmoo) induction, GFP–actin cortical patch localization to the growing mating projection is apparent (Fig. 2 *a–f*). After 90-min incubation, cortical patches in most cells have localized to one pole of the cell, and cells show short projections (Fig. 2 *a* and *b*). After 200-min treatment, the length of the mating projections had increased, but the cortical patches still localized to the tip and side walls of the shmoo (Fig. 2 *c* and *d*). Following prolonged exposure to α-factor (6 hr), the cells had reentered the cell cycle, budding at the end of the shmoo, again localizing cortical patches predominantly to the bud cell (Fig. 2 *e* and *f*). In addition, following the prolonged cell growth arrest, bars of actin–GFP were apparent, reminiscent of those observed in cells bearing the *act1–2* allele (25).

Upon transfer to low nitrogen and carbon medium, diploid cells undergo sporulation, and the distribution of cortical patches can be followed in the spores within the developing ascus (Fig. 2 *g–p*). As the spores form within the outer cell wall, delocalized cortical patches are still apparent, along with a high background fluorescence from the excluded cytoplasm of the spore (Fig. 2 *g–j*). The cortical patches remain in the spores through to spore maturity, although distribution of the patches may vary between individual spores of the same ascus (compare spores in Fig. 2 *l*, *n*, and *p*). These observations are new, since it has not been possible to fix and stain sporulating cells satisfactorily. The most interesting result is that the cortical patches appear to remain within spores through the entire sporulation process.

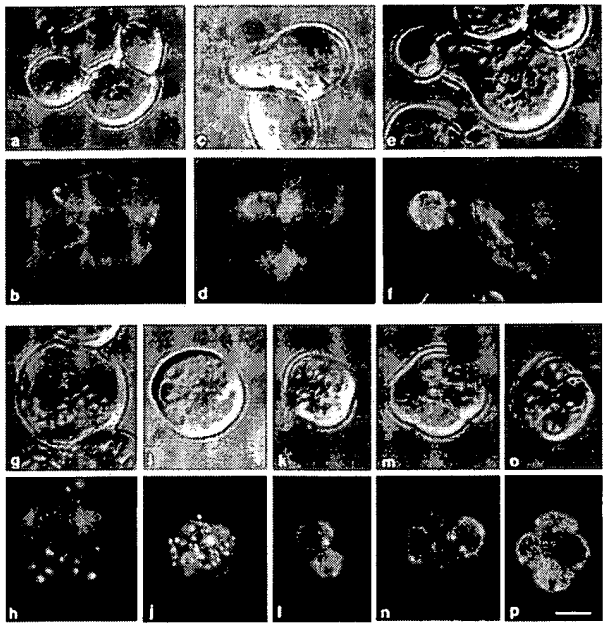

FIG. 2. α-Factor induced shmoo mating projection formation (*a–f*) in *MAT***a** haploid cells, and sporulating diploid yeast cells and asci (*g–p*) showing GFP–actin labeled localization by FITC-filtered UV illumination (*b, d, f, h, j, n–p*). Cortical patch localization is visible in short mating projections by 90 min postaddition of α-factor (*a* and *b*) and the patches remained localized to this projection 200 min postaddition (*c* and *d*) and following reentry into the budding cell cycle 6 hr into the experiment (*e* and *f*). Similarly, cortical patches are clearly visible in spores forming 2 days after transfer into sporulation medium (*g–j*), although not all spores of mature asci (*k–p*) maintain labeled patches. (Bar = 5 μm.)

Expression and Localization of GFP Fusions to Actin Binding Proteins. The yeast actin binding protein Abp1p (26) is also known to localize specifically to cortical actin patches. The yeast fimbrin homologue Sac6p (27) localizes to the cortical patches, as well as the cables, where it acts as a filament bundling protein. To confirm the results obtained with actin–GFP fusions, we made fusions to each of these proteins. The coding sequence for these proteins were amplified by PCR and cloned downstream of the sequence for the increased brightness GFP mutant (S65T) (22) to give pRB2139 (Abp1p) and pRB2140 (Sac6p). Expression of the GFP(S65T)–Abp1p and GFP(S65T)–Sac6p in diploid yeast showed similar localization as the actin–GFP fusions. As expected, the fluorescence was brighter from this construction, although the fluorescent bleaching by the UV illuminating light was significantly faster. Western blot analysis of protein extracts from yeast expressing these fusions using the anti-rGFP antibody (Clontech) showed that in both cases fusion products of the expected sizes are produced.

Since deletion of neither the *SAC6* nor *ABP1* genes is lethal to yeast, determination of the functionality of the fusions was not simply a case of complementing the deletion, as with actin. The *sac6* null mutant is unable to grow at 37°C, and expression of the GFP–Sac6p fusion restored the viability of DDY319 at this temperature, albeit at a reduced level compared with a strain not affected by such elevated temperatures. Neither the actin–$(Ala)_{10}$–GFP or GFP–Abp1p fusions conferred viability at 37°C in this strain. A *sac6 abp1* delete strain is, however, not viable, and this provided another test to determine whether the fusions could complement its deletion. The *sac6* null mutant

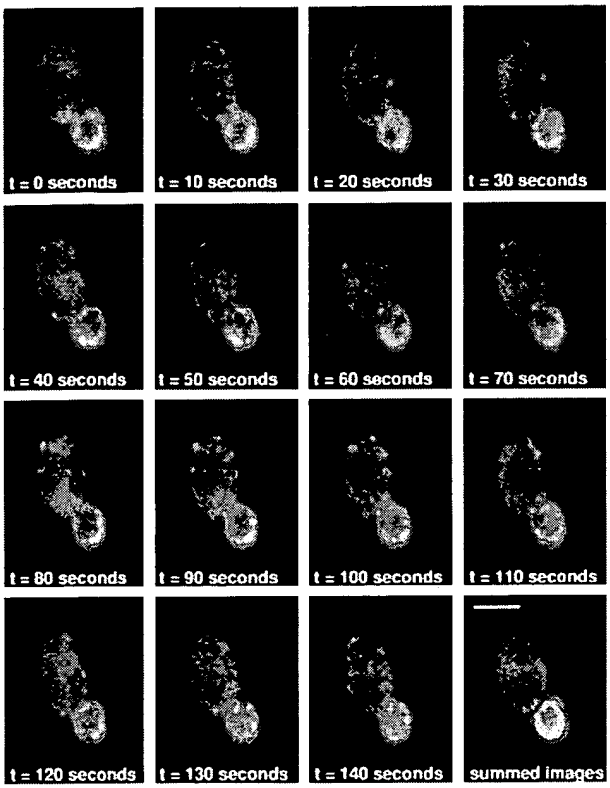

FIG. 3. Sequential images of FITC filter-illuminated yeast cells demonstrating movement of cortical patches between each frame. Patches generally remain localized to the daughter cell in these images, and the patches clearly remain localized to the cell membrane, although patches are free to migrate out of the focal plane observed. Images were digitally captured from a SIT camera at 10-sec intervals, each image representing an average of eight frames taken over 0.25 sec. The final image shows a sum of the GFP–actin localization in the previous 15 frames, and is superimposed on the $t = 0$ sec image, and clearly demonstrates the localization of the patches to the cortical bud cell surface. (Bar = 5 μm.)

strain DDY319 was transformed with either pRB2139 or pRB2140 (GFP–Abp1p or GFP–Sac6p), and the transformants mated with the *abp1* delete strain DDY322. Diploids were selected on SD plates supplimented with histidine, and sporulated. Tetrad dissection and analysis of both transformed diploid strains revealed that the expected ratio of leucine auxotrophs with an absolute requirement for the plasmid, when selected on 5-fluoroorotate (5-FOA) plates. These segregants lack chromosomal copies of both *sac6* and *abp1* and maintained either pRB2139 and pRB2140, confirming that both the expressed fusions are fully functional.

Independently, Waddle *et al.* (28) found that a GFP fusion to Cap2p (another cortical patch-associated protein) similarly localize to the cortical actin patches. The similarity in appearance among all these GFP fusions, and the concordance with expectations based on images of fixed cells, indicates that each of the fusion proteins is labeling at least the cortical actin cytoskeleton faithfully and that these fusions can indeed be used to observe the actin cytoskeleton in living cells and in real time.

Movement of Cortical Actin Patches. The most immediate observation on living cells, and also the most unexpected, was that the cortical actin patches move. They are dynamic structures whose movement is readily visible in real time when viewed under the microscope. Fig. 3 presents a montage of images taken every 10 sec. Although Fig. 3 clearly demonstrates the dynamic nature of the patch movement, time-lapsed movies provide a superior demonstration of this phenomenon, and consequently we have placed a number of representative movies on our World Wide Web home page (see *Materials and Methods* for http address). When living yeast cells are observed under Normarski illumination, small bodies are often observed to move rapidly in the cytoplasm, but direct comparison between Nomarski and FITC-filtered UV illumination showed that these moving bodies represent two populations of dynamic structures; they move at different rates and are not colocalized.

The movement of the actin cortical patches, as observed with actin–GFP, is constrained. Most patches move within a very restricted region of the cell surface. However, occasionally patches are observed to move rapidly across large areas of the cell surface. Because the movement of the patches is not restricted to the focal plane of the microscope, patches can be observed to appear and vanish as they pass through the focal plane. Consequently, it is difficult to estimate the speed of patch movement, but estimates of 0.1–0.5 $\mu m \cdot sec^{-1}$ have been made using GFP fusions to an actin-associated protein Cap2p (28).

Cortical patch movement is also observed using GFP(S65T)–Abp1p and GFP(S65T)–Sac6p. There appear to be no differences observed other than the occasional visualization of filaments with GFP(S65T)–Sac6p. However, it was very difficult to photographs these filaments, and difficult to determine whether they move. Our results on movement with actin–GFP are also entirely consistent with those of Waddle *et al.* (28), who used GFP(S65T)–Cap2p.

Cortical patch movement (as seen using actin–GFP) occurs during all stages of the normal cell cycle, and patches are also observed to move in cells in G_1. Patches continue to move in shmooing cells as the mating projection grows. When cells start sporulating, patches continue moving as the spores start to form, but once the ascus has matured, movement appears to stop. The movement of the cortical patches does not seem to preclude new patch assembly and disassembly. As can be seen in Fig. 4, cortical patches appear to assemble at the opposite cell pole in dividing diploid cells whilst still present at the bud neck, and later disassemble at the bud neck. Observation of this process in a time-lapse movie (see our World Wide Web page) does not indicate a migration of cortical patches between the cell poles, but this cannot be excluded as the patch migration may occur out of the observed focal plane. Further observations and analysis of GFP–actin movement using rapid image capture and three-dimensional reconstitution of images of cells may help address this question.

Effects of Metabolic Inhibitors on Cortical Patch Movement. The rate of cortical patch movement suggests an active process, rather than random movement due to Brownian motion. If so, one might expect that active metabolism might be required to provide energy. To address this question directly, metabolic inhibitors were introduced and their effects on patch movement observed. If patch movement is a result of simple Brownian motion, such poisons should have no effect. Exponentially growing cultures of both

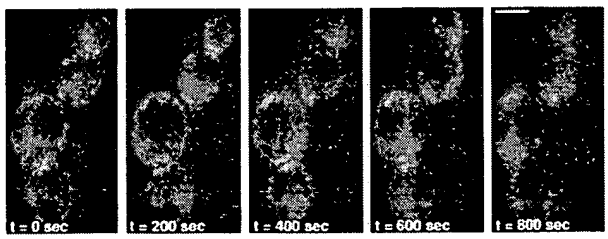

FIG. 4. Sequential images separated temporally by 200-sec intervals demonstrating actin polarization in diploid cells as cortical patches appear on the opposite cell poles, while bud neck localization following cytokinesis still remains apparent, during the entire time course displayed. It is currently unclear whether patches migrate between poles or nascent assembly occurs at the opposite pole. (Bar = 5 μm.)

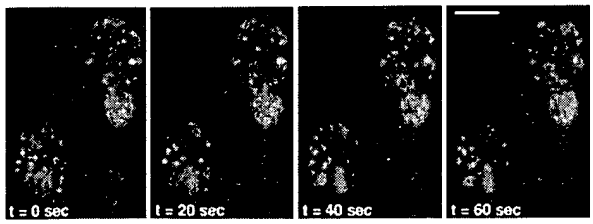

FIG. 5. Sequential images at 20-sec intervals showing reduced cortical patch movement 30 min after the addition of the metabolic inhibitor sodium azide to 20 mM (final concentration) in the diploid yeast DBY5532 expressing the GFP–actin fusion from pRB2133. Direct observation of the cells reveals negligible movement, especially when compared to untreated cells, and although many patches remain stationary, a small population appear to still show movement in the images displayed. (Bar = 5 μm.)

DBY5532 (carrying actin–GFP on pRB2133) and FY23 × FY86 [expressing GFP(S65T)–Abp1p from pRB2139] in defined medium were sampled and treated with 20 mM (final concentration) sodium chloride, sodium fluoride, or sodium azide, or 3.5% (vol/vol, final concentration) formaldehyde, or with no further addition.

Addition of sodium azide caused the movement of the cortical patches to gradually stop over a period of about 45 min but had no other effect on the punctate appearance of the cortical patches (Fig. 5 shows the very slow movement of patches 30 min postazide addition). Sodium fluoride similarly arrested movement, although much quicker, but also caused the patches to become diffuse in appearance; after 5 min the patches had become barely visible and were no longer readily seen by the computer image capture facilities used. Sodium chloride and no treatment had no effect: patches remained visible and moving. Formaldehyde had different effects dependent on the nature of the GFP fusion used. With actin–GFP, the patches stopped moving but remained visible, as with sodium azide. With GFP(S65T)–Abp1p, the patches quickly became faint, as if fluorescence were being quenched.

The results of treatment of the actin–GFP-expressing strains with sodium azide and formaldehyde serve, first of all, as important controls of the movement phenomenon. The movement now cannot be attributed to Brownian motion or instability of the focal plane and other such physical artefacts. The detail that the persistence of fluorescence differs with Abp1p(S65T)–GFP in formaldehyde may simply mean that chromophore of this fusion protein is denatured when that of actin–GFP is still native by this concentration of the agent. These observations also show that energy is required to do the moving, and indeed an issue of considerable interest will be to see how the energy is used. Direct consumption by an actin motor (one of the myosins?) is the most simple and attractive possibility to be investigated, although patch movement may be a result of actin filament treadmilling.

What of the results with sodium fluoride? Sodium azide specifically inhibits cytochrome oxidase in the mitochondria, whereas the fluoride ion inhibits the enolase enzyme of the Embden–Meyerhof pathway. Fluoride combines with phosphate, and the fluorophosphate ion binds magnesium ions, which may make fluoride a less specific inhibitor than the azide ion.

Fusion Protein Localization Within Actin Filaments. Although the cortical actin patches have been visualized in all of the fusions attempted, localization of the fusion proteins to the actin filaments has not yet been possible. Antiactin immunofluorescent microscopy of cells expressing the actin–$(Ala)_{10}$–GFP from pRB2133 shows that the cables are still present and show a normal distribution (data not shown). Attempts to localize the fusion proteins by anti-rGFP immunofluorescent microscopy with the commercially available antiserum have been unsuccessful due to nonspecific background staining. The inability of the actin–GFP fusions to functionally complement the *act1* null mutant might suggest that these fusions are not incorporated into this part of the actin cytoskeleton. However, the ability of the GFP fusion to the actin filament bundling protein Sac6p, a protein that localizes to both cables and patches, to functionally complement the phenotypes associated with a chromosomal deletion of this gene, while not being visually localized to the cables, may reflect other constraints on our ability to visualize the cables *in vivo*.

Potential Roles of Cortical Actin Patch Movement. The movement of the cortical patches may be involved in several processes in the cell. Cortical patches are thought to be cytoplasmic actin cable anchoring points to the cell membrane. If the cables play a role in directing secretory vesicles to the cell membrane in the growing bud (25), movement of the cortical patch, and the associated movement of the attached cable, would allow secretion, and hence membrane addition to the growing cell, to be targeted to different regions of the bud without a metabolically more expensive disassembly/reassembly process. The cortical patches have also been implicated in cell wall morphogenesis (11), and it might be envisioned that as the glucan wall microfibrils are being synthesized at the cortical patches, the patches move to allow the nascent microfibrils to be layered at the area of cell wall generation. In addition, cortical patches have been implicated in endocytosis (8), with two actin-associated proteins (Sac6p and End4p/Sla2p) both playing roles in this process. Whether there are subpopulations of cortical patches performing each of these processes, or if they are each multifunctional is unclear, but the advent of GFP mutants with different spectral properties will allow differential labeling of patch-associated proteins, and make possible their colocalization in living cells.

We thank David Drubin, Fred Winston, and Howard Riezman for yeast strains; Tim Stearns for the GFP-expression plasmids; Roger Tsien and Brendan Cormack for the mutant GFP-bearing plasmids; Sharon Long for the use of the Nikon microscope and SIT imaging system; and David Ehrhardt and Tim Stearns for assistance in its use. This work was supported by grants from the National Institutes of Health (GM46406 and GM46888).

1. Adams, A. E. M. & Pringle, J. R. (1984) *J. Cell Biol.* **98,** 934–945.
2. Kilmartin, J. & Adams, A. E. M. (1984) *J. Cell Biol.* **98,** 922–933.
3. Read, E. B., Okamura, H. H. & Drubin, D. G. (1992) *Mol. Biol. Cell* **3,** 429–444.
4. Hasek, J., Rupes, I., Svobodova, J. & Streiblova, E. (1987) *J. Gen. Microbiol.* **133,** 3355–3363.
5. Gehrung, S. & Snyder, M. (1990) *J. Cell Biol.* **111,** 1451–1464.
6. Ford, S. & Pringle, J. (1986) *Yeast* **2,** S114 (abstr.).
7. Welch, M. D., Holtzman, D. A. & Drubin, D. G. (1994) *Curr. Opin. Cell Biol.* **6,** 110–119.
8. Kübler, E. & Riezman, H. (1993) *EMBO J.* **12,** 2855–2862.
9. Holtzman, D. A., Yang, S. & Drubin, D. G. (1993) *J. Cell Biol.* **122,** 635–644.
10. Raths, S., Rohrer, J., Crausaz, F. & Riezman, H. (1993) *J. Cell Biol.* **120,** 55–65.
11. Mulholland, J., Preuss, D., Moon, A., Wong, A., Drubin, D. & Botstein, D. (1994) *J. Cell Biol.* **125,** 381–391.
12. Prasher, D. C., Eckenrode, V. K., Ward, W. W., Prendergast, F. G. & Cormier, M. J. (1992) *Gene* **111,** 229–233.
13. Chalfie, M., Tu, Y., Euskirchen, G., Ward, W. W. & Prasher, D. C. (1994) *Science* **263,** 802–805.
14. Brand, A. (1995) *Trends Genet.* **11,** 324–325.
15. Pines, J. (1995) *Trends Genet.* **11,** 326–327.
16. Stearns, T. (1995) *Curr. Biol.* **5,** 262–264.
17. Wertman, K. F., Drubin, D. G. & Botstein, D. (1992) *Genetics* **132,** 337–350.
18. Holtzman, D. A., Wertman, K. F. & Drubin, D. G. (1994) *J. Cell Biol.* **126,** 423–432.
19. Kaiser, C., Michaelis, S. & Mitchell, A. (1994) *Methods in Yeast Genetics* (Cold Spring Harbor Lab. Press, Plainview, NY).

20. Sambrook, J., Fritsch, E. F. & Maniatis, T. (1989) *Molecular Cloning: A Laboratory Manual* (Cold Spring Harbor Lab. Press, Plainview, NY).
21. Ma, H., Kunes, S., Schatz, P. J. & Botstein, D. (1987) *Gene* **58,** 201–216.
22. Heim, R., Cubitt, A. B. & Tsien, R. Y. (1995) *Nature (London)* **373,** 663–664.
23. Ng, R. & Abelson, J. (1980) *Proc. Natl. Acad. Sci. USA* **77,** 3912–3916.
24. Cubitt, A. B., Heim, R., Adams, S. P., Boyd, A. E., Gross, L. A. & Tsien, R. Y. (1995) *Trends Biochem. Sci.* **20,** 448–455.
25. Novick, P. & Botstein, D. (1985) *Cell* **40,** 405–416.
26. Drubin, D. G., Miller, K. G. & Botstein, D. (1988) *J. Cell Biol.* **107,** 2551–2561.
27. Adams, A. E., Botstein, D. & Drubin, D. G. (1989) *Science* **243,** 231–233.
28. Waddle, J. A., Karpova, T. S., Waterston, R. H. & Cooper, J. A. (1996) *J. Cell Biol.*, in press.